SoftwareX 19 (2022) 101154

Contents lists available at ScienceDirect

SoftwareX

journal homepage: www.elsevier.com/locate/softx

Original software publication

Interactive software for mapping concentrated displacements in masonry arches

Yu Yuan [a], Gabriel Stockdale [b], Gabriele Milani [a,*]

[a] Department of Architecture, Built Environment and Construction Engineering, Politecnico di Milano, Piazza Leonardo da Vinci, 32, 20133 Milan, Italy
[b] Masonry Methods, Inc., 11034 Crescent Drive, Nevada City, CA 95959, USA

ARTICLE INFO

Article history:
Received 24 December 2021
Received in revised form 27 March 2022
Accepted 20 July 2022

Keywords:
Masonry arch
Homography
Cheap and fast monitoring system
MATLAB GUI

ABSTRACT

Arches are an important part of the masonry architectural heritage and also serve as infrastructure for bridges and culverts. The behavior testing and structural health monitoring of masonry arches require effective measurement methods. There have been a lot of testing methods applied regarding this subject, among which the vision-based non-destructive methods are very appealing. However, as the demands of measuring accuracy and range increase, the labor and economic costs expand to uneconomical levels. A novel, cheap, and fast measurement strategy which focuses directly on the mechanical failure of masonry arches has been developed. This strategy termed Behavior Mapping (BM) is based on homography and does not require a high-precision camera or extensive experimental setup. A scale dry-stack arch was subjected to repeated collapses through springing displacements during the proof-of-concept development of BM. This generated a huge amount of data and required the development of a MATLAB® based graphical user interface (GUI). The objective of this article is to introduce the GUI and the accompanying data for the purpose of providing educational insight into the behavior of masonry arches. These educational experimental cases integrated in the GUI provide the possibility to better understand the failure mechanism of dry-stone arch under foot displacement, as well to easily identify the occurrence of mechanical joints and determine the value of deformations. This GUI can also be adapted for different arch configurations, as well for further real-time monitoring.

Code metadata

Current code version	*V1*
Permanent link to code/repository used of this code version	https://github.com/ElsevierSoftwareX/SOFTX-D-22-00013
Code Ocean compute capsule	*None*
Legal Code License	*MIT License*
Code versioning system used	*None*
Software code languages, tools, and services used	*MATLAB 2021b*
Compilation requirements, operating environments & dependencies	*MATLAB 2021b*
If available Link to developer documentation/manual	*None*
Support email for questions	gabriel@masonrymethods.com

1. Motivation and significance

1.1. Background

Masonry buildings are widely distributed worldwide. They make up a major part of the architectural heritage and many of them are still under service today. As an effective load-bearing structural form, curved masonry members are very important. The behaviors of curved masonry structures still need to be further understood, and data provided by experimental analysis are the basis for furthering this understanding as well as supporting the development of analytical or numerical approaches [1,2]. Additionally, with the existing damages and the sensitivity of the masonry structure itself, investigation and structural health monitoring (SHM) is particularly important for further protection

* Corresponding author.
E-mail address: gabriele.milani@polimi.it (Gabriele Milani).

https://doi.org/10.1016/j.softx.2022.101154

and retrofitting work [3,4]. To meet these requirements, an efficient and economic measurement method is essential. Among the numerous measurement methods, non-destructive testing (NDT) is very appealing. NDT methods include approaches based on liquid penetrant, thermographic, radiographic, ultrasonic, visual tests and so on [5]. Currently, there have been a lot of vision-based technologies applied to masonry arches due to the advantages of simplicity and flexibility [6]. For example, photogrammetry has been applied to collect geometric information and damage distributions of existing buildings [7–11]; and Digital Image Correlation (DIC) has been adopted in laboratories to map full-field displacement, strain and further cracks in masonry structures [12–14]. Naturally, when trying to obtain more refined results, the costs of the measurement and post-processing increase, resulting in uneconomical projects.

A new highly efficient and economical vision-based measurement strategy formulated on the potential rigid-body motions between the blocks of a masonry arch has been introduced [15]. In the preliminary proof-of-concept stage this strategy was applied to a scale model of dry-stone arch that was repeatedly subjected to horizontal springing displacement up to collapse. To deal with the massive data generated, a graphical user interface (GUI) was developed in MATLAB. The GUI synchronizes the video recording of the experimentation with the deformation calculations in both a global and joint specific formats. It allows for the efficient evaluation of the data generated in the experiments and as such provides a great educational opportunity for students interested in understanding and analyzing the mechanical behavior of dry-stone masonry arches subjected to horizontal springing displacements.

1.2. The measurement strategy

The results displayed in the GUI were generated via a novel strategy aimed at monitoring and identifying the mechanical movement of masonry arches. The general strategy is to calculate the fixed set of potential relative movements between two rigid blocks via the application of a 4×4 point grid around each joint. This strategy was then validated by a series of scale arch tests for the preliminary proof of concept stage. The following description of the measurement calculations provides a brief overview of the approach. A comprehensive description can be found in the literature [15].

Based on stability-based design and the rigid-no-tension model, there are eight possible deformations between two blocks. The deformations include rotations (top rotation and bottom rotation), slips (right slip and left slip), and four combinations of the two as shown in Fig. 1. These deformations can be identified through the relative relationship among the vector lengths and dot products of the point sets applied around the joint line. These measurements are achieved by situating the 4×4 grid parallel, perpendicular, and symmetric about the joint line.

As illustrated in Fig. 1, the slip is defined as the relative displacement (δ) of two blocks along the direction of the joint line, which can be easily determined by the Pythagorean theorem in the triangle composed of the original and deformed points grid. The rotation angle can be determined via the dot product of vectors formed by the point sets. Two rotation calculation approaches are applied: (1) dot product calculations between two vectors generated by the same point pairs before and after a deformation; and (2) dot product calculations between two vectors generated after a deformation. Since the result of a dot product is not influenced by the positions of the vectors, the calculation methods can be the same for combined deformations, with slip calculated first and then the potential rotation angle.

Due to the adoption of the 4×4 point grid, there are multiple point pair combinations for vector selections used to calculate a rotation angle or displacement which results in repeated calculations. In total, 16 independent calculations of a slip displacement and 160 independent calculations of a rotation angle are performed. This redundancy is very beneficial for improving the accuracy of the results, especially for angle calculations which are very sensitive to measurement precision.

With the above-mentioned theoretical basis established, the next problem was the extraction of useful information from video recordings for deformation calculations. This was resolved through the application of object tracking. The procedure to gain measurement deformations from a video was established in MATLAB® and summarized below:

(1) Convert the video frames into binary images: During the conversion, the clarity of the grid points in the binary image is improved through a mask based on color thresholds.
(2) Identify and determine the grid points in the initial frame: The circular markers in the converted binary image were filtered via masks based on blob properties.
(3) Track the points from frame to frame: The track can be realized via the MATLAB® Computer Vision Toolbox [16]. The minimum assignment cost identifies the grid points' progression.
(4) Transfer the coordinates: The points are then be projected from the image coordinate plane to the local cartesian plane via a homography transformation [17], which can be easily constructed through the *fitgeotrans* function provided in MATLAB [18].
(5) Perform deformations calculation: All the calculations are performed instantaneous as discussed above, and the deformation type can then be ascertained via the variance of the variable, which will be exemplified in Section 3.1.

The more detailed measurement principles and validations are described in the literature [15]. This article's objective is to present the wealth of data generated in the development of the proof of concept for the behavior mapping of masonry arches for educational purposes.

1.3. Scale arch tests

To assist in the validation and demonstrate the effectiveness of the measurement strategy, the mechanical failure processes of a scale model of dry-stone arch subjected to horizontal springing displacement were recorded. The scale arch was composed of 11 identical blocks manufactured via 3D printing, with a clear span of 268 mm and a rise of 81 mm. Sandpaper sheets were glued on the lateral surfaces of the blocks to preclude any sliding. A mask with the measuring points was glued on the surface of each block. The detailed dimensions of the arch and applied points grid are shown in Fig. 2.

The mechanical failure of the arch was triggered by a horizontal displacement applied manually at the right foot and referenced by rulers. The left foot remained translationally fixed. The failure propagation was recorded via a cell phone camera positioned at three different locations to the arch (see Fig. 2). A total of six tests were performed, four at point A and one at both points B and C. The data generated from these tests were integrated into the GUI. For a more detailed description of the experimental setup and execution refer to the literature [15].

2. Software description

2.1. Software architecture

With the application of the introduced strategy, a large number of coordinates of the marked grid points were recorded

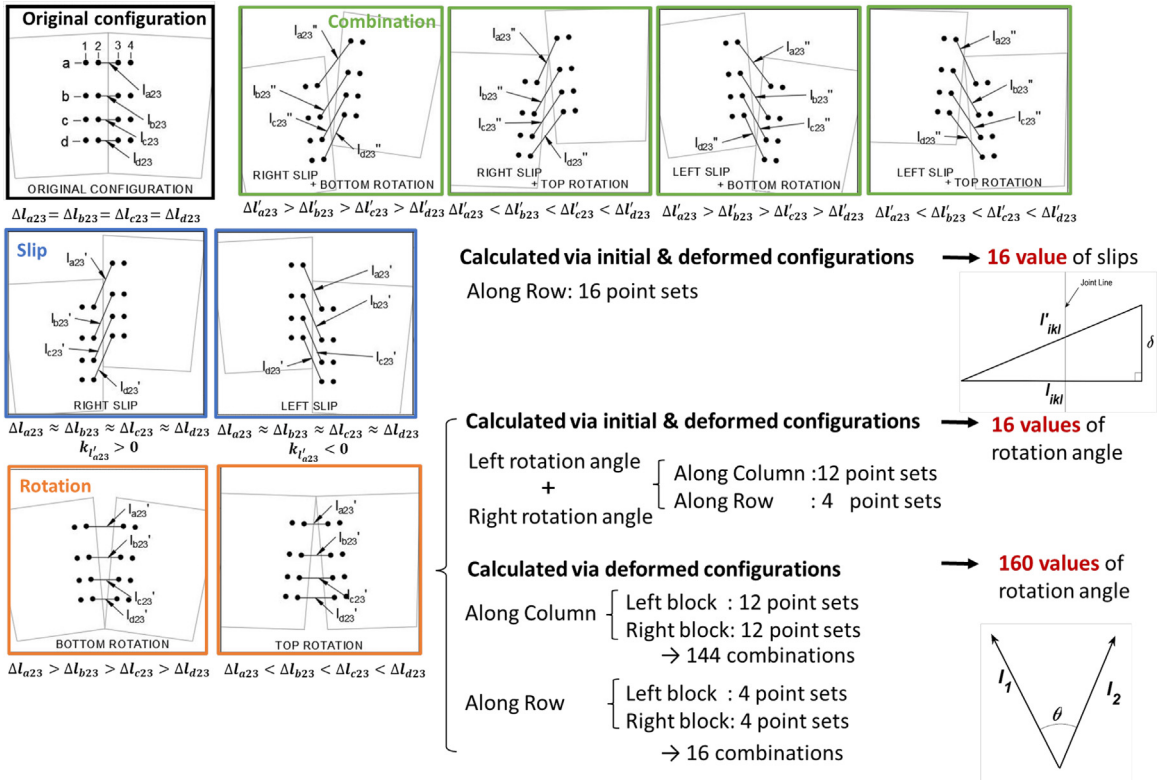

Fig. 1. Identification and calculation strategy of rigid block deformations.

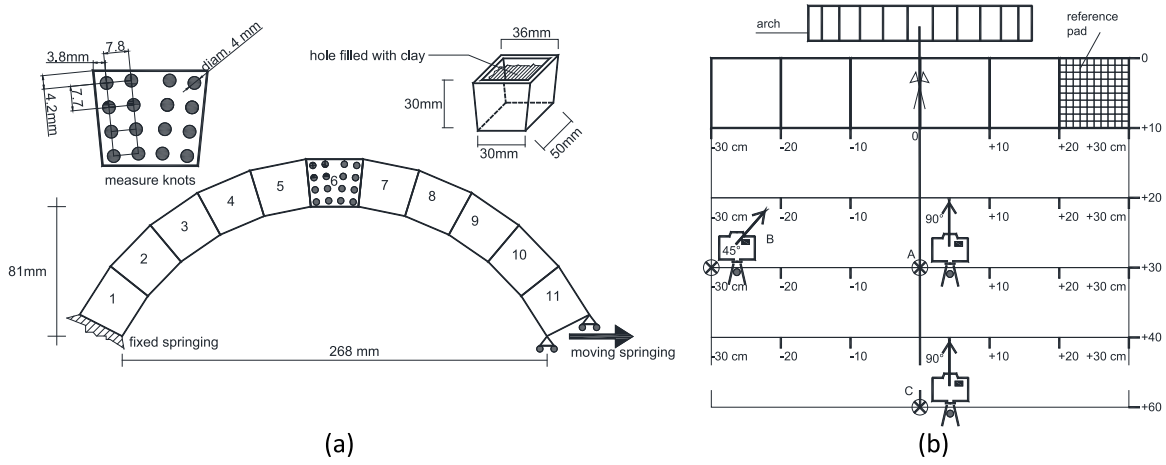

Fig. 2. Experimental scheme for scale arches: (a) dimensions of blocks and arch; (b) positions of camera.

throughout the failure procedure (i.e., 16 points per joint and 10 joints for the tested arch). In addition to the rotations and slip deformations of a joint, another type of intuitive indicator for mechanical failure can also be useful, that is the lengths of symmetric point pairs about the joint. The average length of outer point sets (i.e., points of columns 1 and 4 in Fig. 1) is named as ID length 1, and the inner (i.e., points of columns 2 and 3 in Fig. 1) as ID length 2 separately.

As shown in Fig. 3, the user can select the test and the measurement results to be displayed through the following interactive components (indicated by the solid frames):

(1) Drop down menu 1: Select the test number to load into the interface
(2) Drop down menu 2: Select the type of measurement results to examine
(3) Joint button: Switch between the global results (unpressed) as shown in Fig. 3(a), and the more detailed joint specific results (pressed, Fig. 3(b)) as shown in Fig. 3(b)
(4) Switch button: Play and pause the video
(5) Slider: Track and/or select the currently displayed frame

With the different selections of the user, the plot window and data table (indicated by the dashed frames) will respond with different displays:

(1) Plot window 1: displays the current frame of the selected test; or plays the video if the 'switch button' is at 'play';
(2) Plot window 2: displays the specified measurement results of all the joints of the selected test; or displays the measurement results and its variance of one joint when a joint button is pressed. The vertical black dashed line bar

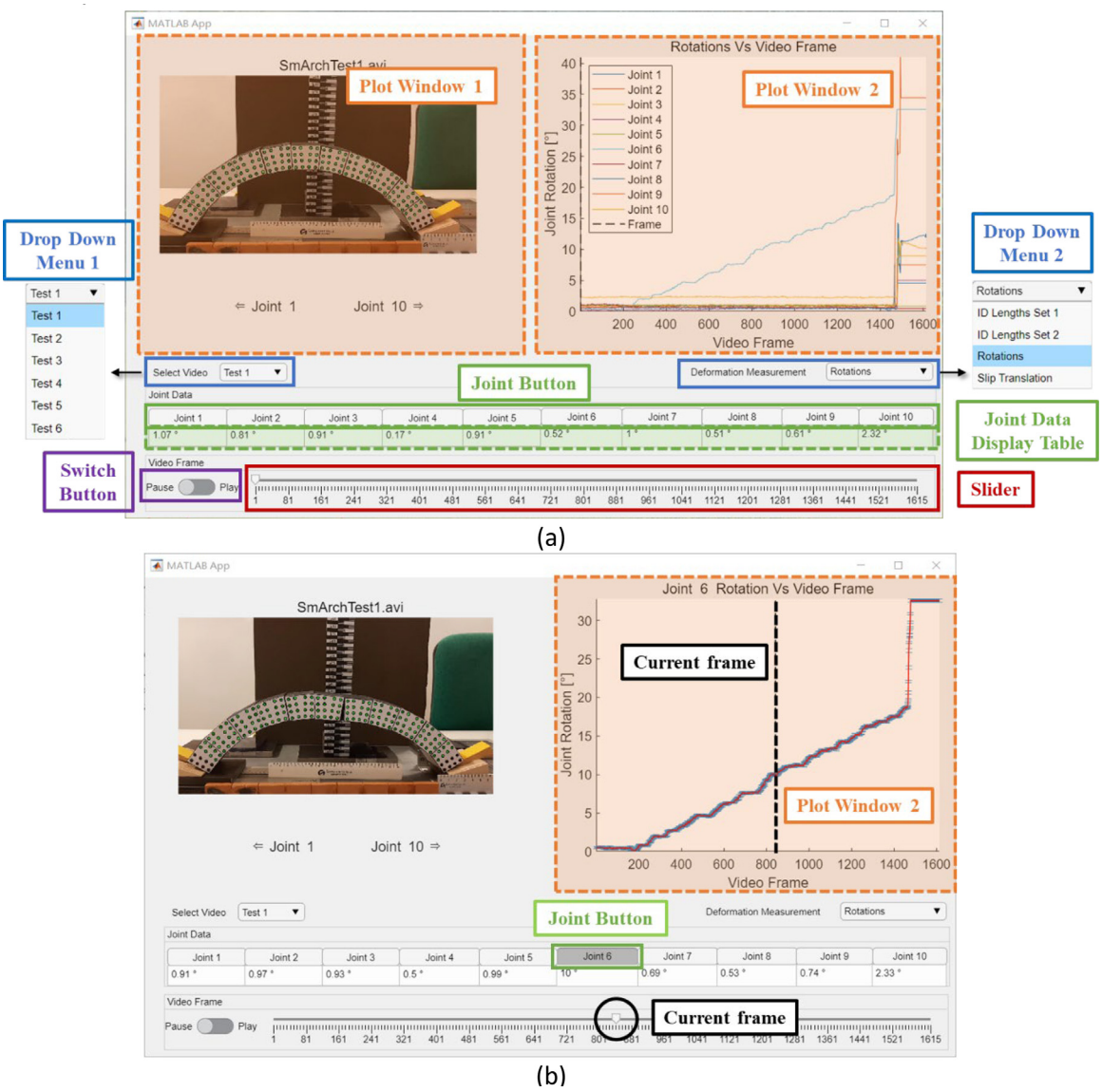

Fig. 3. Layout of the GUI: (a) initial interface; (b) interface with a joint button pressed.

indicates the position of the current frame in plot window 1;

(3) Joint data display table: displays the measurement results of each joint under the current frame.

2.2. Software functionalities

The GUI introduced in this article aims for the users to conveniently determine the deformation values, as well to better understand the formation of mechanical joints of a masonry arch. The results of six tests were integrated into the GUI code directly. For including additional tests adopting the same measurement strategy, it is necessary to add or replace the path of files when programming the GUI code, including the video, and a MATLAB data file that stores the deformation calculations obtained from the behavior mapping in a specific order [15]. Users can choose to display the deformation of all joints until failure, or to display the deformation and variance of a specific joint, form which the mechanical joints and deformation type can be distinguished. It was necessary to develop this GUI to store and display these large amounts of data in a practical order and allow users to conveniently view and critically examine the results. In summary, the following functions can be achieved, and some examples will be put forward in the next section:

(1) Determine the mechanical joints and the deformation type of the arch under mechanical failure.
(2) Determine the deformation values (rotation or slip) of each joint at any time from the joint table, or by clicking a certain point on curves in 'plot window 2'.
(3) Recognize the moment and configuration of the collapse of the arch from the video or deformation curves.

3. Illustrative examples

3.1. Determination of mechanical joints and deformations

The mechanical joints can be easily recognized from either the video or the deformation plot of all the joints. As shown in Fig. 4(a), joint 6 (indicated by light blue line) has obvious changes in all deformation plots as compared to the other joints. Even when the opening of joints is not visually apparent from the video, the deformation values were accurately recorded in the table and curves. While for the non-mechanical joints, both the

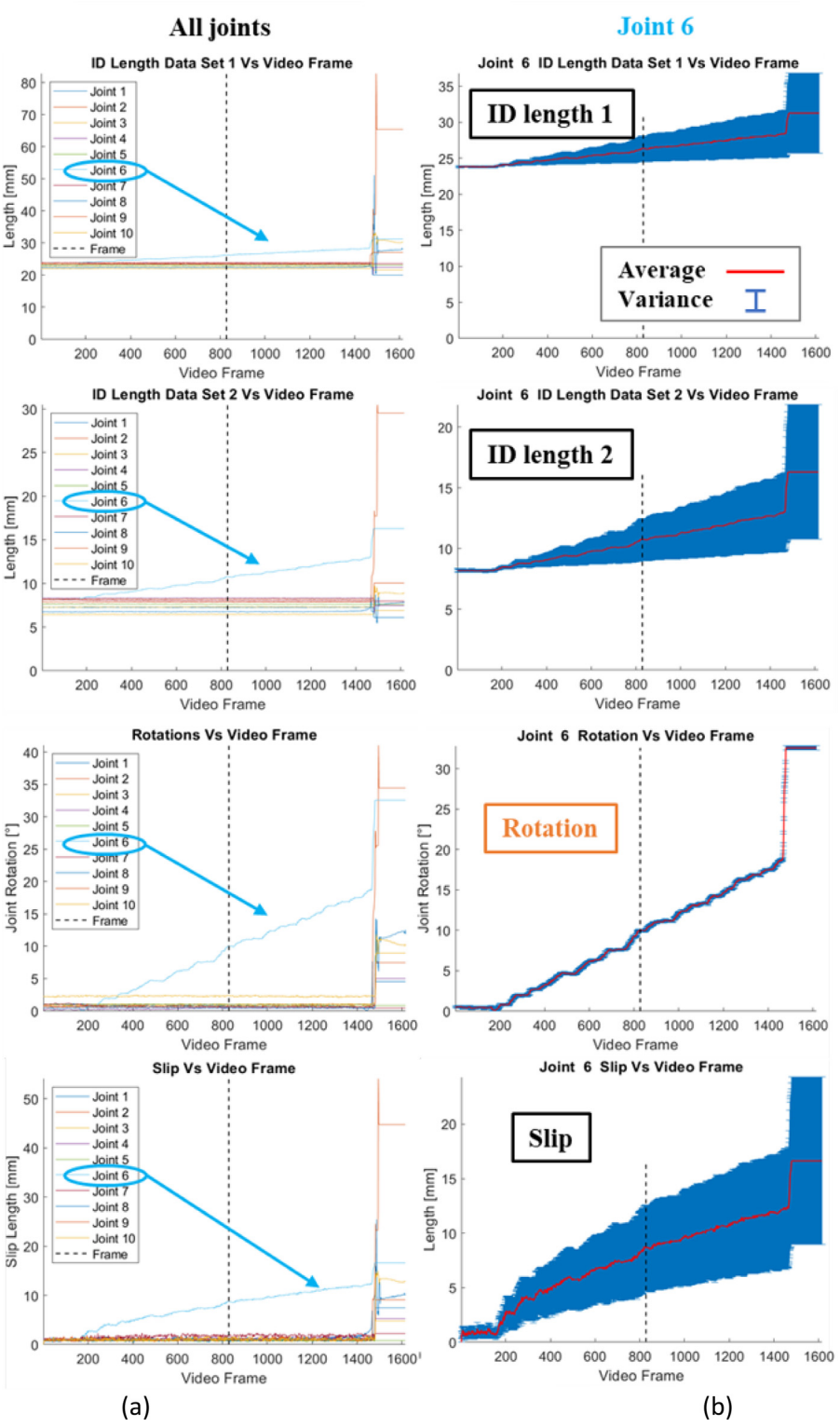

Fig. 4. Example of identification of mechanical joints and deformation type: Deformation vs. frame plots for (a) all joints and (b) joint 6 of test 1.

deformation value and variance will stay around a constant value. The exact deformation values can be read from the data display table for each joint, or by clicking a certain point on the curves the deformation value and frame number will be shown. It should be noted that the general MATLAB® functionality of the plot window is preserved in the GUI interface. Thus the plots can be zoomed and dragged to facilitate the observation of more details of the video or curves.

Once the mechanical joints are recognized, the deformation type of the joint can be identified by comparing the deformation curves of this single joint. As shown in Fig. 4(b), it can be determined that the deformation type of joint 6 is a rotation. This conclusion is drawn because the variance (indicated by blue bars) of the rotation measurements is constant while the other deformation types sustain continued increases to their

Table 1
Identification of mechanical joints via the introduced GUI.

Stable	Failure
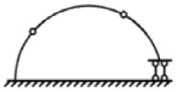	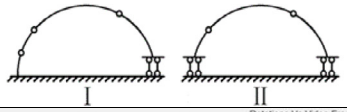
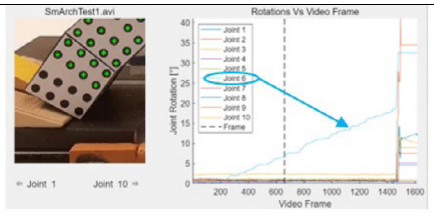	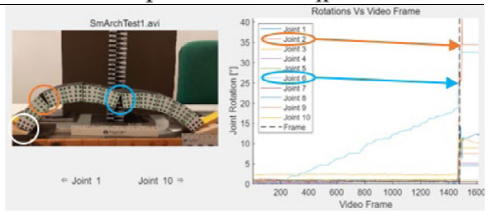
Test 1: Joint 0 & Joint 6	Joint 2 & Joint 6 & Joint 0 (II)
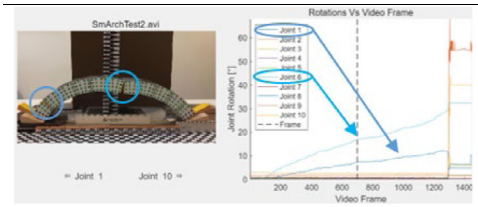	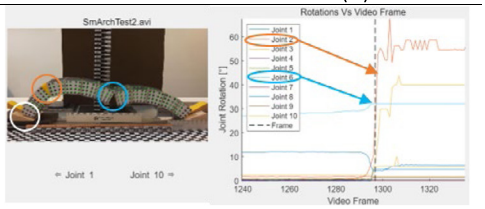
Test 2: Joint 1 & Joint 6	Joint 2 & Joint 6 & Joint 0 (II)
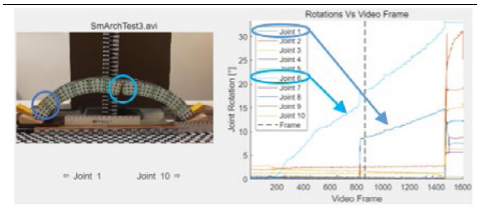	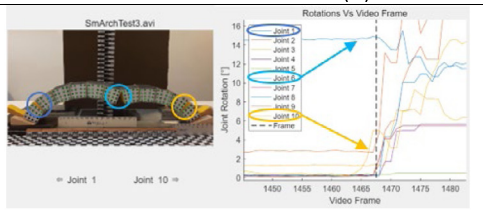
Test 3: Joint 1 & Joint 6	Joint 1 & Joint 6 & Joint 10 (I)
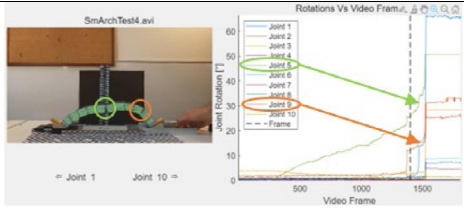	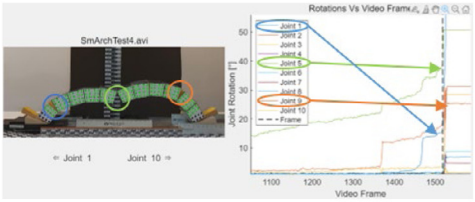
Test 4: Joint 5 & Joint 9	Joint 1 & Joint 5 & Joint 9 (I)
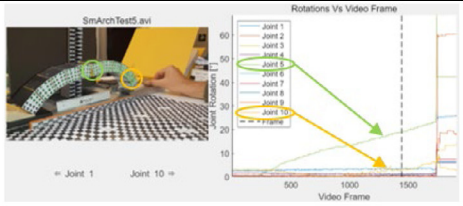	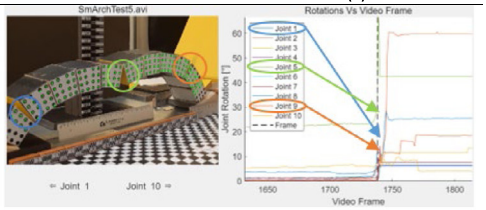
Test 5: Joint 5 & Joint 10	Joint 1 & Joint 5 & Joint 9 (I)
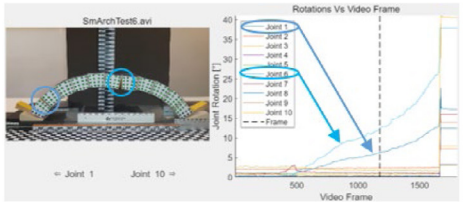	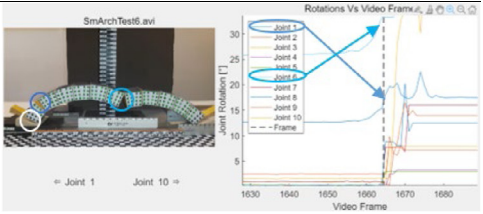
Test 6: Joint 1 & Joint 6	Joint 1 & Joint 6 & Joint 0 (II)

variance throughout the test. This indicates the inaccuracy of the calculations and identifies the measurements as erroneous.

3.2. Identification of the mechanical failure

From the perspective of structural mechanics, the typical failure of an arch is the formation of four hinges which leads to the loss of stability of the structural system [19,20]. In the scale arch tests, a horizontal displacement was applied at the right foot to trigger the failure. Considering that the slide between blocks was precluded by the experimental settings, to adapt to the increase of the springing before complete collapse there has to be two hinges opening at intrados and extrados separately. This condition when the arch can still stand even with some joints

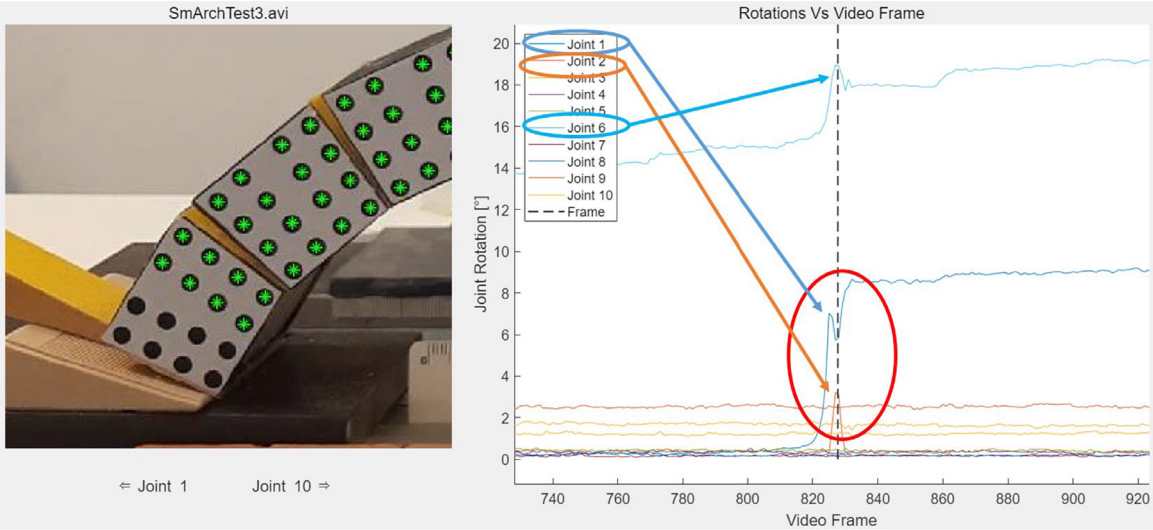

Fig. 5. The transformation of mechanical joints in test 3.

open is referenced as 'stable' in Table 1. When a third hinge opens (referenced as 'failure I' in Table 1) or the left foot moves as well (referenced as 'failure II' in Table 1), then the system will no longer be stable. The schematic diagrams of stable and failure situations are shown in Table 1.

The failure of the arch can happen very quickly and without obvious warning signs to the transition from the 'stable' status, but the GUI allow the frame by frame evaluation of the mechanical joints. The zoom function of the plot window also provides convenience for more detailed examinations of the video and data. Combining this with the thorough deformation curves provides a very comprehensive arch behavior analysis model. For each test, two frames respectively showing stable and failure statuses are summarized in Table 1. For test 2, two hinges can be directly identified via the deformation curves from the beginning of the test. In the remaining tests only one hinge appeared in the early stages of settlement. By observing the enlarged video, it can be noticed that the left arch foot has rotated, forming another rotation hinge denoted as 'Joint 0'. By playing the video frame by frame around the moment when a sudden deformation appeared in a certain joint, it can be observe that after the second hinge appeared in the arch, the first block rotated back to its original position.

The time of failure can be easily located through the indicating bar on the plots through the huge rise of curves around the failure. The mechanical joint that finally caused collapse does not necessarily appear in the previous development of failure. For example, in test 2 as referenced from Table 1 it can be seen that when the collapse is approaching, the blue line (representing joint (1) dropped, while the orange line (representing joint (2) increased quickly. In the video, it shows that block 2 has rotated, and the mechanical joint has shifted from joint 1 to joint 2. After the failure of the arch, the measurement curves show some deformations that are inconsistent with the movement of the blocks from the video. The failure occurs so quickly that the measurement method can no longer accurately track the marked points, resulting in erroneous calculations.

The real-time calculations corresponding to the video frame provide very detailed behavior of the tested arch. As indicated by the red circle in Fig. 5, the small deformation (rotation less than 5 degrees) of joint 2 (indicated by the orange line) in a short period of time can also be recorded and reflected in the plots. The rotation deformations of joint 1 and joint 2 exhibit opposite behavior at the selected frame, since they are both caused by the movement of the second block. Another example of test 5 is shown in Fig. 6(a) where the rotation increasement of mechanical joint 10 was not as obvious as in other tests. Here the rotation value of this joint first decreased before it increased. Combined with the enlarged video, it can be found that there is an unclosed opening at joint 10 when the arch is placed at the initial position. The direction of the rotation angle was not marked with a sign; thus, the original opening needed to be compensated first when rotation happened. A similar situation also appeared in test 3.

4. Impact

The GUI introduced in this article provides a convenient approach to evaluate deformations calculated via a novel measurement strategy designed for masonry arches. The novelty of the measurement strategy lies in the characterization for mechanical failure of the masonry arch at the joints. Together with the application of homography, the approach provides the possibility of monitoring through a limited number of markers and a single camera. The development of the deformations and the occurrence of mechanical joints can be easily recognized from the GUI as well as the detailed values including deformations, variance and time. Through the simultaneous presentation of video and the deformation plots, the users can study and explore detailed behaviors of a dry-stone arch subjected to horizontal springing displacements. This results in the GUI holding educational significance for engineers interested in masonry arch behavior.

On the basis of this GUI, the results display can also be easily adapted for masonry arches with different configurations. For this current version, the results were integrated into the code of the GUI directly, but there is also the possibility of transforming the same platform into a real-time monitoring GUI after the full integration with the video tracking and deformation calculating aspects. In this application prospect, the development of this GUI is necessary for the large amount of data that will appear.

5. Conclusions

This article introduced a GUI for presenting mechanical deformations of a scale masonry arch subjected to repeated collapses from horizontal springing displacement recorded via a novel measurement strategy. This strategy is a vision-based non-destructive method that can identify and quantify mechanical deformations between rigid blocks via point grids marked on

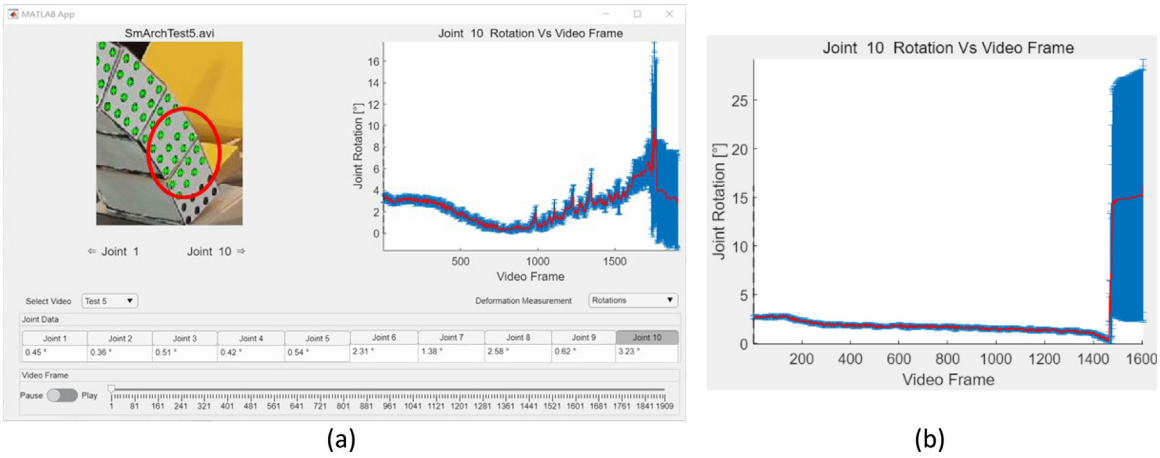

Fig. 6. Rotation of joint 10 of (a) test 5 and (b) test 3.

the block surface. The GUI allows the users to easily check the results and learn the mechanism of the dry-stone arch. With the complexity of failure of masonry arch systems, this GUI serves as a valuable resource for young researchers and students to begin their studies on the matter. The potential of this strategy to serve as a cheap and fast monitoring system for existing masonry arches also exists and extends the significance of the GUI as the foundation of a monitoring interface and warning system for real-time monitoring for different arch configurations in the future.

Declaration of competing interest

The authors declare that they have no known competing financial interests or personal relationships that could have appeared to influence the work reported in this paper.

Acknowledgments

Yu Yuan would like to acknowledge the financial support provided by the Chinese Scholarship Council (CSC) for performing her Phd program at Polytechnic University of Milan, Milan, Italy.

Appendix A. Supplementary data

Supplementary material related to this article can be found online at https://doi.org/10.1016/j.softx.2022.101154.

References

[1] Sarhosis V, de Santis S, de Felice G. A review of experimental investigations and assessment methods for masonry arch bridges. Struct Infrastruct Eng 2016;12:1439–64.
[2] Stockdale G. Generalized processing of FBG/FRP stain data for structural health monitoring. 2012.
[3] Grillanda N, Milani G, Ghosh S, Halani B, Varma M. Shm of a severely cracked masonry arch bridge in India: Experimental campaign and adaptive NURBS limit analysis numerical investigation. Construct Build Mater 2021;280:122490. http://dx.doi.org/10.1016/j.conbuildmat.2021.122490.
[4] Stockdale G. Reinforced stability-based design: a theoretical introduction through a mechanically reinforced masonry arch. Int J Masonry Res Innov 2016;1:101. http://dx.doi.org/10.1504/IJMRI.2016.077469.
[5] Bergamo O, Campione G, Donadello S, Russo G. In-situ NDT testing procedure as an integral part of failure analysis of historical masonry arch bridges. Eng Failure Anal 2015;57:31–55. http://dx.doi.org/10.1016/j.engfailanal.2015.07.019.
[6] Feng D, Feng MQ. Computer vision for SHM of civil infrastructure: From dynamic response measurement to damage detection – a review. Eng Struct 2018;156:105–17. http://dx.doi.org/10.1016/j.engstruct.2017.11.018.
[7] Armesto J, Arias P, Roca J, Lorenzo H. Monitoring and assessing structural damage in historic buildings. Photogrammetr Rec 2008;23:36–50. http://dx.doi.org/10.1111/j.1477-9730.2008.00466.x.
[8] Riveiro B, Caamaño JC, Arias P, Sanz E. Photogrammetric 3D modelling and mechanical analysis of masonry arches: An approach based on a discontinuous model of voussoirs. Autom Construct 2011;20:380–8. http://dx.doi.org/10.1016/j.autcon.2010.11.008.
[9] Solla M, Caamaño JC, Riveiro B, Arias P. A novel methodology for the structural assessment of stone arches based on geometric data by integration of photogrammetry and ground-penetrating radar. Eng Struct 2012;35:296–306. http://dx.doi.org/10.1016/j.engstruct.2011.11.004.
[10] Riveiro B, Solla M, de Arteaga I, Arias P, Morer P. A novel approach to evaluate masonry arch stability on the basis of limit analysis theory and non-destructive geometric characterization. Autom Construct 2013;31:140–8. http://dx.doi.org/10.1016/j.autcon.2012.11.035.
[11] Kassotakis N, Sarhosis V, Peppa MV, Mills J. Quantifying the effect of geometric uncertainty on the structural behaviour of arches developed from direct measurement and structure-from-motion (SfM) photogrammetry. Eng Struct 2021;230:111710. http://dx.doi.org/10.1016/j.engstruct.2020.111710.
[12] Dhanasekar M, Prasad P, Dorji J, Zahra T. Serviceability assessment of masonry arch bridges using digital image correlation. J Bridge Eng 2019;24:04018120. http://dx.doi.org/10.1061/(ASCE)BE.1943-5592.0001341.
[13] Acikgoz S, DeJong MJ, Soga K. Sensing dynamic displacements in masonry rail bridges using 2D digital image correlation. Struct Control Health Monit 2018;25:e2187. http://dx.doi.org/10.1002/stc.2187.
[14] Ribeiro D, Cal¸cada R, Ferreira J, Martins T. Non-contact measurement of the dynamic displacement of railway bridges using an advanced video-based system. Eng Struct 2014;75:164–80. http://dx.doi.org/10.1016/j.engstruct.2014.04.051.
[15] Stockdale G, Yuan Y, Milani G. The behavior mapping of masonry arches subjected to lumped deformations. Construct Build Mater 2022;319:126069. http://dx.doi.org/10.1016/j.conbuildmat.2021.126069.
[16] Szeliski R. Computer vision. London: Springer London; 2011, http://dx.doi.org/10.1007/978-1-84882-935-0.
[17] Artin E. Geometric algebra. Interscience Publishers; 1957.
[18] Hartley R, Zisserman A. Multiple view geometry in computer vision. Cambridge University Press; 2004, http://dx.doi.org/10.1017/CBO9780511811685.
[19] Stockdale G, Milani G, Sarhosis V. Increase in seismic resistance for a full-scale dry stack masonry arch subjected to hinge control. Key Eng Mater 2019;817:221–8. http://dx.doi.org/10.4028/www.scientific.net/KEM.817.221.
[20] Galassi S, Misseri G, Rovero L, Tempesta G. Failure modes prediction of masonry voussoir arches on moving supports. Eng Struct 2018;173:706–17. http://dx.doi.org/10.1016/j.engstruct.2018.07.015.